NATURAL FREQUENCIES AND OPEN–LOOP RESPONSES OF AN ELASTIC BEAM FIXED ON A MOVING CART AND CARRYING AN INTERMEDIATE LUMPED MASS

S. Park

Mechatronics Research Team, Research Institute of Industrial Science and Technology (RIST), San 32, Hyoja-dong, Namku, Pohang, Korea and Robotics Laboratory, School of Mechanical Engineering, POSTECH, Korea

W. K. Chung and Y. Youm

School of Mechanical Engineering, Pohang University of Science and Technology (POSTECH), San 31, Hyoja-dong, Namku, Pohang, Korea

and

J. W. Lee

Department of Mechanical Engineering, Yeungnam University, 21-4, Dae-dong, Kyeongsan, Korea

(*Received* 30 *November* 1998, *and in final form* 6 *August* 1999)

In this paper, the motion of a Bernoulli–Euler cantilever beam clamped on a moving cart and carrying an intermediate lumped mass is considered. The equations of motion of the beam–mass–cart system are analyzed through unconstrained modal analysis, and a unified characteristic equation for calculating the natural frequencies of the system is established. The changes of natural frequencies and the corresponding mode shapes with respect to the changes in the ratios between the beam mass, the lumped mass and the cart mass and to the concentrated position of the lumped mass are investigated with the frequency equation, which can be generally applied to this kind of system. The exact and assumed-mode solutions including the dynamics of the base cart are obtained, and the open-loop responses of the system by arbitrarily designed forcing functions are given by numerical simulations. The results match well with physical phenomena even in the extreme cases where the mass is attached to the bottom and to the top of the beam.

© 2000 Academic Press

1. INTRODUCTION

There has been a lot of research work on the vibration analysis of flexible structures or flexible beams subject to various boundary and load conditions. One kind of such beam–mass systems considered in a vast number of previous studies is a uniform cantilever beam which carries a concentrated mass or body at one end and the other end is fixed or restrained to a large inertial frame or the ground [1–6].

Bhat and Wagner [1] obtained the exact frequency equations for a uniform cantilever carrying a slender tip mass whose center of gravity did not coincide with the attachment point. Anderson [2] obtained the frequency equation for a cantilever with an asymmetrically attached tip mass. Parnell and Cobble [3] solved the displacement equation for a uniform cantilever beam with a concentrated mass at one end using the Laplace transform under generally distributed lateral load and arbitrary boundary and initial conditions. Laura *et al.* [4] determined natural frequencies and modal shapes of a clamped-free beam which carried a finite mass at the free end. Gürgöze [5] determined the approximate fundamental bending eigenfrequency of a restrained cantilever beam carrying a tip heavy body. He also derived the frequency equation of a clamped-free beam with tip mass when a spring-mass system was attached to it [6].

The other type of the beam-mass system considered is a uniform beam carrying a concentrated mass or system of masses located at an arbitrary position along the beam [7–15]. Chen [7] formulated and solved the problem of vibration of a simply supported beam carrying a mass concentrated at the middle span of the beam. Goel obtained the natural frequencies with respect to the change of the ratio between the beam mass and the concentrated mass for the beam which was free at one end with the other end hinged by a rotational spring [8], and both ends were restrained by rotational springs [9]. Amba-Rao [10] obtained a closed-form solution for solving the problem of free vibration of a partially fixed beam with unequal end fixities and carrying an arbitrary number of concentrated masses in an arbitrary way. Pan [11] solved the vibrational motion of a simply supported and fixed-free beam carrying a system of heavy bodies. Stanišić and Hardin [12] developed a theory describing the motion of a beam under an arbitrary number of moving masses. Maurizi and Bellés compared the fundamental frequency of a simply supported beam with a concentrated mass suited at an arbitrary point along the beam by Bernoulli–Euler and Timoshenko theories [13]. They also determined the fundamental frequency according to Timoshenko's theory for the case of a uniform cantilever beam with an arbitrarily located mass [14]. Low [15] obtained the explicit frequency equations of a beam carrying a concentrated mass for various boundary conditions by dividing the beam into two parts at the point where the concentrated mass was attached and considering continuity conditions at the point.

All the above studies, however, dealt with beam–mass systems where at least one part of the beams was fixed or restrained at a large inertial frame, and thus ignored the dynamics of the base frame. When a flexible beam carrying a concentrated mass is fixed on a moving cart, and if the beam mass and the concentrated masses can no longer be negligible compared with that of the cart, the motion of the beam–mass system affects that of the cart, and vice versa. In this case, therefore, all the dynamics of the beam, the concentrated mass and the cart should be considered simultaneously to obtain the characteristics of the vibrational motion of the system.

For example, when reclaimers in automated warehouses, forklift cars or ladder cars carry heavy loads from a high place to another place, vibrational motions due to the flexibility of the main beam are unavoidable, even though they have truss-structured beams. Furthermore, when the load moves along the flexible beam, the natural frequencies of the beam and the vibrational motion vary along the

position of the load. Therefore, to analyze the total motion of the beam–mass–cart system, the rigid body motion of the cart as well as the vibrational motion of the beam–mass system should be included in the analysis. Models similar to this beam–mass–cart system can be found in civil and military airplane wings designed to carry heavy external stores along their span and in antennas operated in space [16].

Concerning the researches on the vibrational behavior of flexible beams attached to a moving base, To [17] calculated natural frequencies and mode shapes of a mast antenna structure, but he modelled it as a cantilever beam with base excitation and tip mass because the total mass of the beam–mass system is negligible compared with that of the base. Ge *et al.* [18] presented asymptotically stable end-point regulators for a flexible beam fixed on a moving base and carrying a lumped tip mass, and simulated their performances utilizing the constrained modal analysis. Park *et al.* [19] obtained equations of motion, frequency equations and exact solutions of the motion of a flexible beam fixed on a moving cart and carrying a lumped tip mass using unconstrained modal analysis. Garcia and Inman [20] considered servo stiffness as well as natural boundary conditions to find eigenfunctions and the corresponding eigenvalue equations of a single-link flexible beam that was undergoing slewing motion at an actively controlled pinned end, while the other end was free. The vibration of flexible beams attached to moving supports has been also studied for vibration analysis and active control of robotic manipulators with elastic links [21–25].

The target of this research is the modelling and motion analysis of a Bernoulli–Euler beam fixed on a moving cart and carrying a concentrated mass attached to an arbitrary position along the beam. Another purpose of this research is to obtain a general unified frequency equation for the beam–mass–cart system and to investigate the change of natural frequencies and the corresponding mode shapes with respect to the changes in mass ratios of the system and to the changes of the position of the concentrated mass. The exact and assumed-mode solutions including the dynamics of the base cart are obtained, and the open-loop responses of the beam–mass–cart system by an arbitrarily designed forcing function are also given.

In the following section the equations of motion of the beam–mass–cart system is derived, and the frequency equation is described in section 3. Numerical simulations to obtain the open-loop responses of the system are reported in section 4, followed by the conclusions.

2. EQUATIONS OF MOTION

Figure 1 shows the beam–mass–cart system considered in this study. The elastic beam is assumed to follow the Bernoulli–Euler beam model and to be clamped tightly on the moving cart.

The elastic beam with a concentrated mass at its mid-span can be considered as two sub-beams divided by the mass [15]. In this paper, however, the δ-function [8–12] is adopted to represent the effect of the mass concentrated at an arbitrary position along the flexible beam. The equation of motion and the boundary
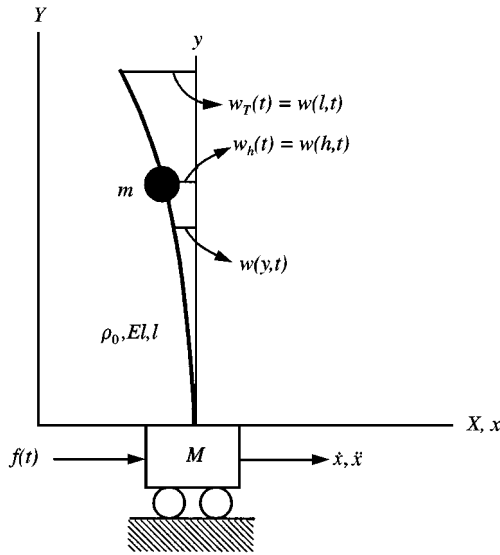
Figure 1. The beam–mass–cart system considered.

conditions of the beam–mass–cart system in Figure 1 are derived by Hamilton's, principle as follows [26]:

$$M\ddot{x} + \int_0^l [\rho_0 + m\delta(y - h)](\ddot{x} + \ddot{w})\,\mathrm{d}y = f(t), \tag{1}$$

$$EIw'''' + [\rho_0 + m\delta(y - h)](\ddot{x} + \ddot{w}) = 0, \tag{2}$$

$$w(0, t) = w'(0, t) = EIw''(l, t) = EIw'''(l, t) = 0, \tag{3}$$

where M is the mass of the cart, m is the mass of the concentrated mass, l is the length of the elastic beam, ρ_0 is the mass per unit length of the elastic beam without concentrated mass, EI is the flexural rigidity of the unloaded beam, x is the position of the cart, $w(y, t)$ is the deflection of the beam at y, and $\delta(y - h)$ is the *Dirac δ-function*. In the above equations, dots denote differentiations with respect to time and primes denote differentiations with respect to the spatial co-ordinate y.

As a special case of the beam–mass–cart system shown in Figure 1, if the lumped mass is concentrated at the tip of the beam, the effect of the lumped mass is included in the boundary conditions, and thus the equations of motion and the boundary conditions can be represented as follows:

$$M\ddot{x} + m(\ddot{x} + \ddot{w}_T) + \rho_0 \int_0^l (\ddot{x} + \ddot{w})\,\mathrm{d}y = f(t), \tag{4}$$

$$EIw'''' + \rho_0(\ddot{x} + \ddot{w}) = 0, \tag{5}$$

$$w(0, t) = 0, \qquad w'(0, t) = 0,$$

$$EIw''(l, t) = 0, \qquad EIw'''(l, t) = m(\ddot{x} + \ddot{w}_T), \tag{6}$$

where $w_T(t) = w(l, t)$ is the deflection at the tip of the beam.

3. MODAL ANALYSIS

3.1. UNCONSTRAINED MODAL ANALYSIS

Analyzing equations (1) and (2) by forcing $\ddot{x}(t)$ to zero is the *constrained modal analysis*. In this paper, for the exact modal analysis, the equations of motion are analyzed utilizing the *unconstrained modal analysis* [25, 27] without forcing $\ddot{x}(t)$ to zero. Hence, the position of the cart, $x(t)$, can be assumed to have a solution of the form

$$x(t) = \alpha(t) + \beta q(t), \tag{7}$$

where $\alpha(t)$ describes the motion of the center of mass, and the deflection of the beam at y, $w(y, t)$, is assumed to have a solution of the form

$$w(y, t) = \phi(y)q(t). \tag{8}$$

Then, the motion of the center of mass without perturbation can be obtained as

$$M_t \ddot{\alpha}(t) = f(t) \tag{9}$$

if β satisfies

$$\beta = -\frac{m}{M}\psi(h) - \frac{\rho_0}{M}\int_0^l \psi(y)\,dy, \tag{10}$$

where $M_t = M + m + m_b$ is the total mass of the beam–mass–cart system, $m_b = \rho_0 l$ is the mass of the flexible beam, and

$$\psi(y) \triangleq \beta + \phi(y). \tag{11}$$

On the other hand, substitution of equations (7) and (8) into equation (2) yields

$$EI\psi''''(y)q(t) + [\rho_0 + m\delta(y - h)]\psi(y)\ddot{q}(t) = -[\rho_0 + m\delta(y - h)]\ddot{\alpha}(t). \tag{12}$$

To get the normal mode solutions, where the effect of the external force vanishes, one can decompose equation (12) into two equations as follows:

$$\ddot{q}(t) + \omega^2 q(t) = 0, \tag{13}$$

$$EI\psi''''(y) - \omega^2[\rho_0 + m\delta(y - h)]\psi(y) = 0, \tag{14}$$

where ω is the natural frequency of the beam–mass–cart system, and the boundary conditions in equation (3) become

$$\psi(0) = \beta, \quad \psi'(0) = 0, \quad \psi''(l) = 0, \quad \psi'''(l) = 0. \tag{15}$$

The Laplace transform of equation (14), considering equation (15), leads to the following equation:

$$\bar{\psi}(s) = \frac{s^3}{s^4 - k^4} \beta + \frac{s}{s^4 - k^4} \psi''(0) + \frac{\psi'''(0)}{s^4 - k^4} + \frac{mw^2\psi(h)}{EI} \frac{e^{-hs}}{s^4 - k^4}, \tag{16}$$

where $\bar{\psi}(s)$ represents the transformed function of $\psi(y)$ and

$$k^4 = \rho_0\omega^2/EI. \tag{17}$$

The inverse Laplace transform of equation (16) gives the general solution of equation (14) as follows:

$$\psi(y) = \frac{\beta}{2}(\cos ky + \cosh ky) - \frac{\psi''(0)}{2k^2}(\cos ky - \cosh ky) - \frac{\psi'''(0)}{2k^3}(\sin ky - \sinh ky)$$

$$- \frac{m\omega^2\psi(h)}{2EIk^3} U(y - h)[\sin k(y - h) - \sinh k(y - h)], \tag{18}$$

where $U(y - h)$ is a unit step function at $y = h$. The constants $\psi''(0)$ and $\psi'''(0)$ can be obtained from the last two boundary conditions of equation (15) as follows:

$$\psi''(0) = \frac{m\omega^2\psi(h)}{2EIk} \frac{1}{1 + \cos kl \cosh kl} \{[\cos k(l - h) + \cosh k(l - h)](\sin kl + \sinh kl)$$

$$- [\sin k(l - h) + \sinh k(l - h)](\cos kl + \cosh kl)\} + \beta k^2 \frac{\sin kl \sinh kl}{1 + \cos kl \cosh kl} \tag{19}$$

and

$$\psi'''(0) = -\frac{m\omega^2\psi(h)}{2EI} \frac{1}{1 + \cos kl \cosh kl} \{[\cos k(l - h) + \cosh k(l - h)]$$

$$\times (\cos kl + \cosh kl) + [\sin k(l - h) + \sinh k(l - h)](\sin kl - \sinh kl)\}$$

$$- \beta k^3 \frac{\cos kl \sinh kl + \sin kl \cosh kl}{1 + \cos kl \cosh kl}. \tag{20}$$

Thus, from equations (18)–(20), $\psi(y)$ is obtained as

$$\psi(y) = A(y)\psi(h) + B(y)\beta, \tag{21}$$

where

$$A(y) = \frac{m\omega^2}{4EIk^3} \left\{ \frac{\cos ky - \cosh ky}{1 + \cos kl \cosh kl} [(\sin k(l - h) + \sinh k(l - h))(\cos kl + \cosh kl) \right.$$

$$- (\cos k(l - h) + \cosh k(l - h))(\sin kl + \sinh kl)]$$

$$+ \frac{\sin ky - \sinh ky}{1 + \cos kl \cosh kl} [(\sin k(l - h) + \sinh k(l - h))(\sin kl - \sinh kl)$$

$$+ (\cos k(l - h) + \cosh k(l - h))(\cos kl + \cosh kl)]$$

$$\left. - 2U(y - h)[\sin k(y - h) - \sinh k(y - h)] \right\}, \tag{22}$$

and

$$B(y) = \frac{1}{2} \left[\cos ky + \cosh ky - \frac{\sin kl \sinh kl}{1 + \cos kl \cosh kl} (\cos ky - \cosh ky) \right.$$

$$\left. + \frac{\cos kl \sinh kl + \sin kl \cosh kl}{1 + \cos kl \cosh kl} (\sin ky - \sinh ky) \right]. \tag{23}$$

Integration of equation (2) with respect to y and substitution of equation (1) into the resulting equation give

$$M\ddot{x} + EIw'''(0, t) = f(t). \tag{24}$$

When $f(t) = 0$, substitution of equations (7), (8) and (13) into equation (24) yields

$$\beta = \frac{EI}{M\omega^2} \phi'''(0) = \frac{EI}{M\omega^2} \psi'''(0). \tag{25}$$

From equations (20) and (25), β is obtained as

$$\beta = C\psi(h) + D\beta, \tag{26}$$

where

$$C = -\frac{m}{2M}\frac{1}{1+\cos kl\cosh kl}\{[\cos k(l-h)+\cosh k(l-h)](\cos kl+\cosh kl)$$

$$+[\sin k(l-h)+\sinh k(l-h)](\sin kl-\sinh kl)\}, \tag{27}$$

and

$$D = -\frac{\rho_0}{Mk}\frac{\sin kl\cosh kl+\cos kl\sinh kl}{1+\cos kl\cosh kl}. \tag{28}$$

Then, equations (21) and (26) give

$$\psi(y) = \left[A(y)+\frac{C}{1-D}B(y)\right]\psi(h) \triangleq F(y)\psi(h). \tag{29}$$

3.2. THE FREQUENCY EQUATION

Equation (29), when $y = h$, gives the following equation:

$$[1-D-A(h)+A(h)D-B(h)C]\psi(h) = 0. \tag{30}$$

Since $\psi(h) = 0$ yields a trivial solution, the inner part of the bracket in equation (30) must vanish. From this condition, after some mathematical manipulations, the frequency equation is obtained as follows:

$$1+\cos\xi\cosh\xi$$

$$+\frac{r_1}{4}[\cos\xi\cosh(\xi-2\eta)+\cos(\xi-2\eta)\cosh\xi+\sin\xi\sinh(\xi-2\eta)$$

$$-\sin(\xi-2\eta)\sinh\xi+2\cos\xi\cosh\xi+4\cos\eta\cosh\eta]$$

$$+\frac{r_2}{\xi}(\sin\xi\cosh\xi+\cos\xi\sinh\xi)$$

$$+\frac{r_3\xi}{4}[2\sin(\xi-\eta)\cosh(\xi-\eta)-2\cos(\xi-\eta)\sinh(\xi-\eta)+2\cos\eta\sinh\eta$$

$$-2\sin\eta\cosh\eta+\cos(\xi-2\eta)\sinh\xi-\sin\xi\cosh(\xi-2\eta)$$

$$+\cos\xi\sinh\xi-\sin\xi\cosh\xi] = 0, \tag{31}$$

where $r_1 = m/M$, $r_2 = m_b/M$, $r_3 = m/m_b$, $\xi = kl$ and $\eta = kh$.

Equation (31) is general and can be applied to find the frequency equation of this kind of beam–mass system. For example, if the concentrated mass is located at the tip, then $\xi = \eta$; if the mass is attached to the bottom of the flexible beam, then $\eta = 0$,

and consequently, the last term on the left-hand side of equation (31) vanishes. If the flexible beam carries no concentrated mass, then $r_1 = 0$ and $r_3 = 0$, and if one end of the flexible beam is fixed at a large inertial frame, i.e., $M \rightarrow \infty$, then $r_1 = 0$ and $r_2 = 0$.

Table 1 shows several cases of the beam–mass system, appropriate conditions in equation (31) and the resulting frequency equations. In Table 1, the frequency equation for the first system is a well-known one for the fixed-free beam without lumped mass. The frequency equation of the second system in Table 1 is also obtained by solving the equations of motions of the sixth system, equation (4)–(6), with constrained modal analysis [19]. The frequency equation of the third system in Table 1 is exactly the same with the result by Low [15] under the same boundary conditions. This equation can also be obtained by solving the beam–mass–cart system in Figure 1 by the constrained mode expansion method by letting $\ddot{x}(t)$ be zero in equations (1) and (2). The frequency equation of the fifth system is the same as that of the fourth system if the base mass, M, in the fourth system becomes $m + M$. The frequency equation of the sixth system in Table 1 is obtained by solving equations (4)–(6) using the same method described in the previous subsection [19].
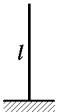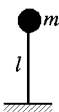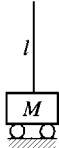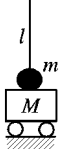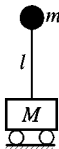
The modelling of the fourth system in Table 1 is similar to modelling a slewing structure with an elastic beam attached to a joint having rotational inertia. The eigenfrequencies of a slewing elastic beam are between those of a pinned-free beam and a clamped-free beam [20]. The frequency characteristics of the beam–mass–cart system are also changed with respect to the changes in the mass ratios and the position of the concentrated mass. The elastic beam considered in this study is clamped on the moving cart which is free to move without friction. In this case, in general, the open-loop behavior of the system appears between that of a clamped-free beam and sliding-free beam [33]. For example, if the concentrated mass and the beam mass are very small compared with the mass of the cart, the frequency equation of the system will approach that of a clamped-free beam. The same result will be obtained if the friction and/or the gear ratio between the moving cart and wheel shafts of the cart become very large. On the contrary, if the beam mass becomes dominant, the frequency characteristic of the system shows that of a sliding-free beam.

There are many research results on the change of natural frequencies with respect to the change of the ratio between the beam mass and the concentrated mass [1, 2, 5, 6, 8, 10, 12–15, 17, 22, 25, 28, 31, 32, 34]. Libresu [16] also obtained the change of the damped frequency with respect to the change of the ratio between the beam mass and the concentrated mass for various mass position. In this study, however, the effect of all the mass ratios, r_1, r_2 and r_3, and the change in position of the concentrated mass to the frequency equation of the beam–mass–cart system were considered. The roots of the frequency equation (31) were obtained numerically by utilizing the *Newton–Rapson method* with respect to the changes in position of the concentrated mass for various mass ratios, r_1 and r_2, and Figure 2 shows the first five eigenfrequencies of the equation.

As shown in Figure 2, natural frequencies become lower as r_1 increases with respect to the same position of the concentrated mass. However, as the position of the concentrated mass is changed, the eigenfrequencies increase and decrease

TABLE 1

Frequency equations for various beam–mass systems and comparative studies

System	Conditions	Resulting frequency equation	Earlier studies
	$r_1 = 0$ $r_2 = 0$ $r_3 = 0$	$1 + \cos\xi\cosh\xi = 0$	Garcia and Inman [20], Ankarali and Diken [23], Barbieri and Özguner [25]
	$r_1 = 0$ $r_2 = 0$ $\xi = \eta$	$1 + \cos\xi\cosh\xi$ $+ r_3\xi(\cos\xi\sinh\xi$ $- \sin\xi\cosh\xi) = 0$	Bhat and Wagner [1], Laura *et al.* [4] Gürgöze [5] Park *et al.* [19] Fung and Shi [24], Liu and Huang [28], Stephen [29]
	$r_1 = 0$ $r_2 = 0$	$1 + \cos\xi\cosh\xi$ $+ \frac{r_3\xi}{4}[2\sin(\xi - \eta)\cosh(\xi - \eta)$ $- 2\cos(\xi - \eta)\sinh(\xi - \eta)$ $- 2\sin\eta\cosh\eta + 2\cos\eta\sinh\eta$ $+ \cos(\xi - 2\eta)\sinh\xi$ $- \sin\xi\cosh(\xi - 2\eta)$ $+ \cos\xi\sinh\xi - \sin\xi\cosh\xi] = 0$	Maurizi and Bellés [14], Low [15], Gürgöze [30], Hamdan and Shabaneh [31], Hamdan and Dado [32]
	$r_1 = 0$ $r_3 = 0$	$1 + \cos\xi\cosh\xi$ $+ \frac{r_2}{\xi}(\sin\xi\cosh\xi + \cos\xi\sinh\xi) = 0$	Garcia and Inman [20], Barbieri and Özguner [25], Blevins [33]
	$\eta = 0$	$1 + \cos\xi\cosh\xi + r_1(1 + \cos\xi\cosh\xi)$ $+ \frac{r_2}{\xi}(\sin\xi\cosh\xi + \cos\xi\sinh\xi) = 0$	
	$\xi = \eta$	$1 + \cos\xi\cosh\xi + 2r_1\cos\xi\cosh\xi$ $+ \frac{r_2}{\xi}(\cos\xi\sinh\xi + \sin\xi\cosh\xi)$ $+ r_3\xi(\cos\xi\sinh\xi - \sin\xi\cosh\xi) = 0$	Ge *et al.* [18], Park *et al.* [19], Low [22]

repeatedly. In that case, there are the same number of nodal points, at which the frequencies of the beam with a concentrated mass match those of the beam without concentrated mass, with the number of modes. In the case of a simply supported beam which carries a concentrated mass, the eigenfrequencies are symmetric with respect to the middle point of the beam [35]. Increasing r_2, on the other hand, makes the beam more stiff, and thus the frequency deviation with respect to increasing r_1 is reduced.
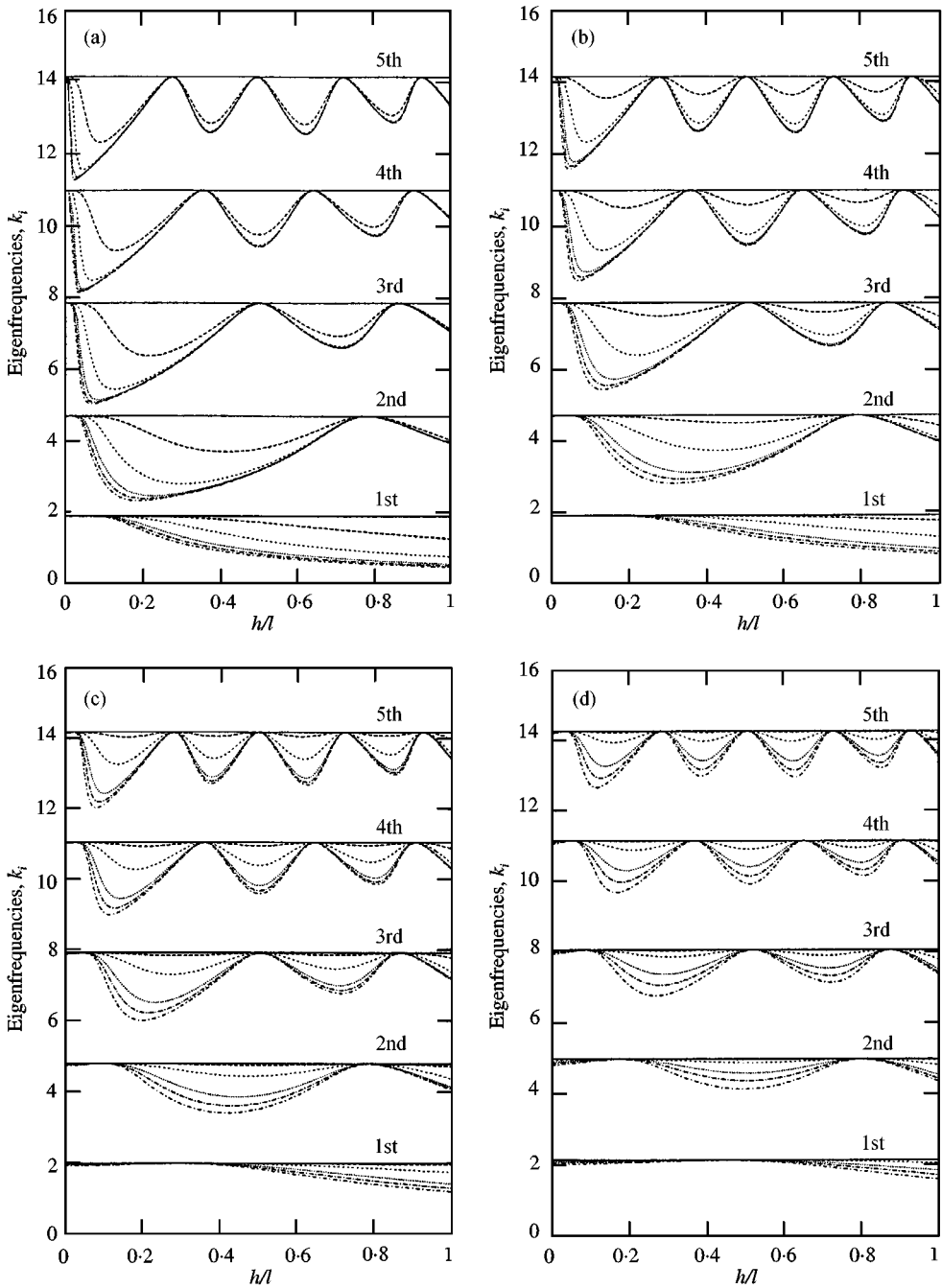
Figure 2. The first five roots of the frequency equation (31) with respect to the change of the position of the concentrated mass for various mass ratios, r_1 and r_2: (a) $r_2 = 0.01$, (b) $r_2 = 0.1$, (c) $r_2 = 0.5$, (d) $r_2 = 2$. —, $r_1 = 0$; --, $r_1 = 0.01$; ---, $r_1 = 0.1$; $\cdots$, $r_1 = 0.5$; $\cdot-\cdot-$, $r_1 = 1$; $\cdot-\cdot-$, $r_1 = 2$.

Chai and Low [36] showed that weights placed at the bottom ($h/l = 0$) have no effect on the frequency: namely, the ratio of natural frequencies between the loaded and unloaded beam is constant. However, as seen in Figure 2, the differences in
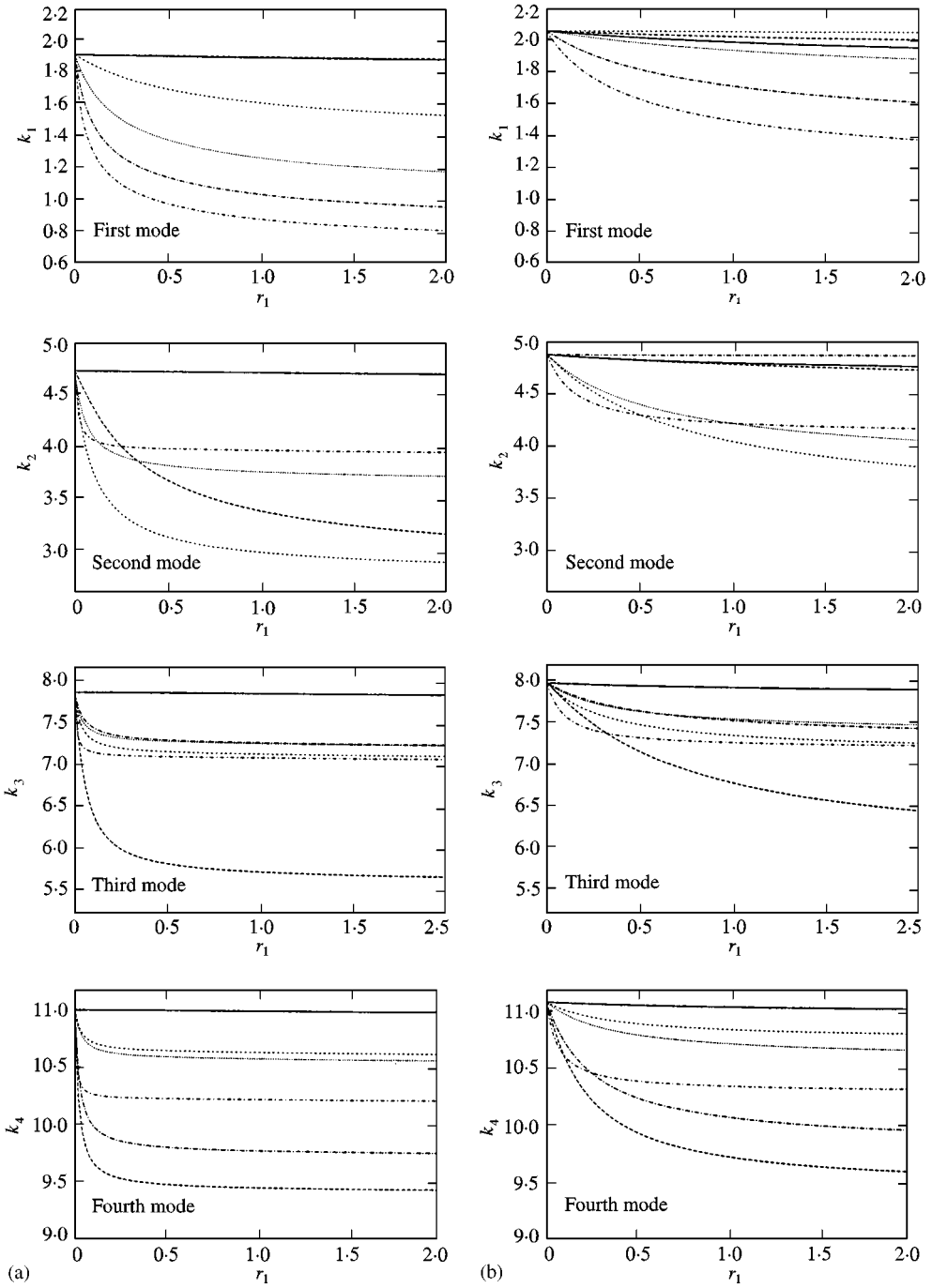
Figure 3. The first four roots of the frequency equation (31) with respect to the change of the mass ratio r_1 for various positions of the concentrated mass: (a) $r_2 = 0.1$, (b) $r_2 = 1$. ——, $h/l = 0$; ― ―, $h/l = 0.2$; - - -, $h/l = 0.4$; ·····, $h/l = 0.6$; ― · ―, $h/l = 0.8$; ― · · ―, $h/l = 1$.

natural frequencies between the loaded and unloaded beam near $h/l = 0$ become large as r_1 increases, especially at large r_2. This result is due to the effect of the mass ratio r_1 which is not considered in reference [36]. As seen in Table 1, the increase in the concentrated mass, m, increases r_1 in the fifth system or, equivalently, the base mass in the fourth system, and the natural frequencies decrease as r_1 or the base mass increases as reported in reference [22].

Figure 3 shows the first four mode solutions of the frequency equation (31) with respect to the changes in the mass ratios, r_1 and r_2, for various values of h/l. In Figure 3, it can be seen that the frequencies become lower as r_1 increases. However, the frequencies do not show any correspondence with respect to varying h/l because the eigenfrequencies increase and decrease repeatedly as h/l varies as shown in Figure 2. Comparing the results in (a), $r_2 = 0.1$, and (b), $r_2 = 1$, the frequency deviation gets smaller as r_2 increases, mainly at lower eigenfrequencies. This shows that the effect of the lumped mass on the natural frequencies of the beam becomes smaller, especially at lower frequency modes, if the beam becomes stiff.

The frequency equation by the unconstrained modal analysis, equation (31), was compared with that by a constrained one, the frequency equation of the third system in Table 1, and Figure 4 shows the difference between the two methods. In Figure 4, the cart mass and beam mass were given as 10 and 1 kg respectively, and the concentrated mass was changed from 0 to 20 kg at (a) $h/l = 0.5$ and (b) $h/l = 1$. As seen in Figure 4, the differences in natural frequencies between the two methods become more significant as the mass ratio increases, especially near the first mode, although the difference between the two methods is negligible at higher modes as reported in reference [25].

Using the obtained frequency equation, the mode shapes are derived in the next subsection.

3.3. MODE SHAPES

If a function $\rho(y)$ is defined as

$$\rho(y) \triangleq \rho_0 + m\delta(y - h), \tag{32}$$

the orthogonality condition is given as follows (see Appendix A):

$$\int_0^l \rho(y)\psi_i(y)\phi_j(y)\,\mathrm{d}y = \delta_{ij}, \tag{33}$$

where δ_{ij} is the *Kronecker delta*. From the orthogonality condition in equation (33), $\psi_i(h)$ is obtained as (see Appendix B)

$$\psi_i(h) = \frac{1}{\left\{ m\left(1 - \dfrac{C_i}{1 - D_i}\right) + \rho_0 \displaystyle\int_0^l F_i(y)\left[F_i(y) - \dfrac{C_i}{1 - D_i}\right]\mathrm{d}y \right\}^{1/2}} \tag{34}$$
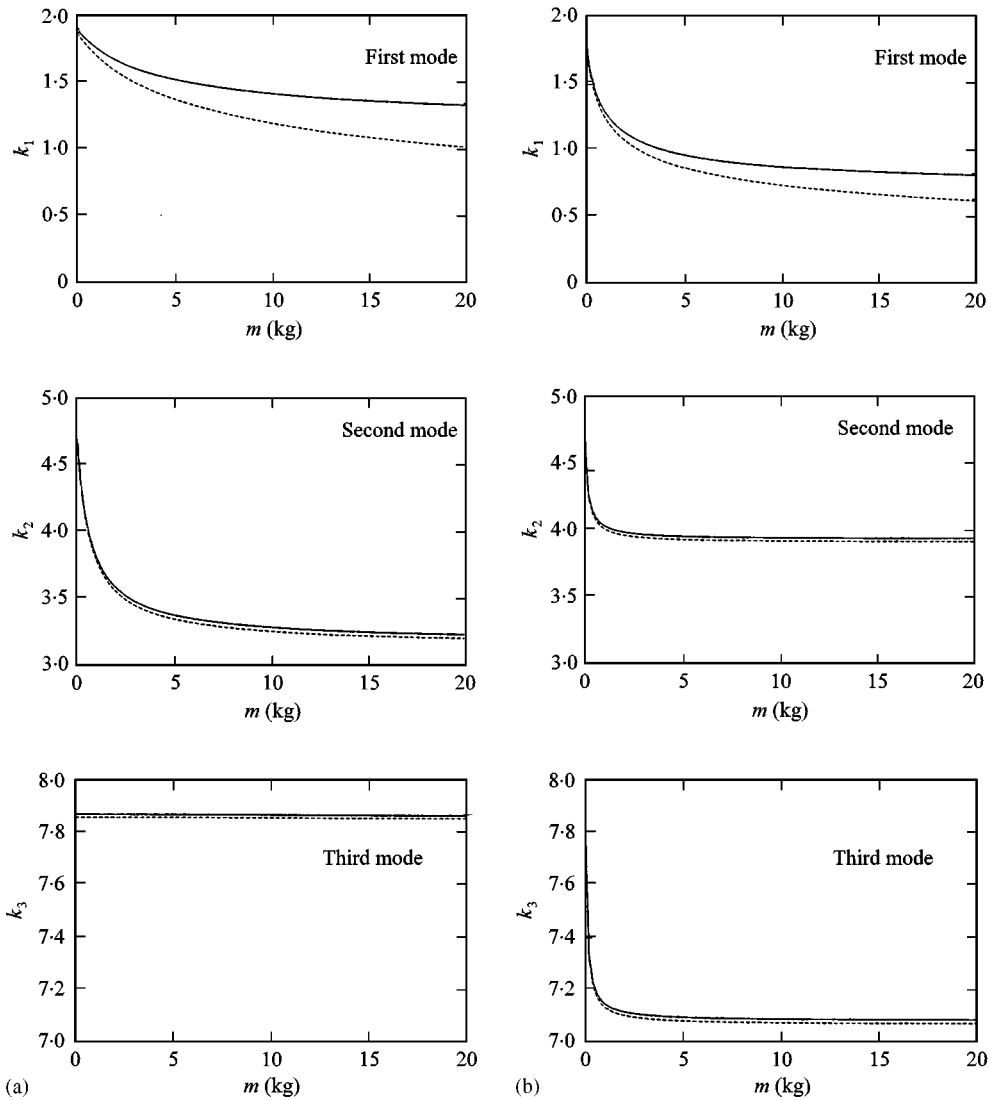
Figure 4. Comparison of the first three roots of the frequency equation by the unconstrained method, equation (31), with the constrained method, the third equation in Table 1, with respect to the change of the concentrated mass at $M = 10$kg, $m_b = 1$kg: (a) $h/l = 0.5$, (b) $h/l = 1$. ——, unconstrained method; – –, constrained method.

Then, $\psi_i(y)$ and β_i for given k_i are obtained from equations (29) and (26) respectively.

Figure 5 shows the normalized mode shapes, $\phi_i(y) = \psi_i(y) - \beta_i$, corresponding to the first five modes of the frequency equation (31) when the system parameters listed in Table 2 are used.

The effects of the changes in the mass ratio r_1 on mode shapes were considered and Figure 6 shows five normalized mode shapes corresponding to the first five
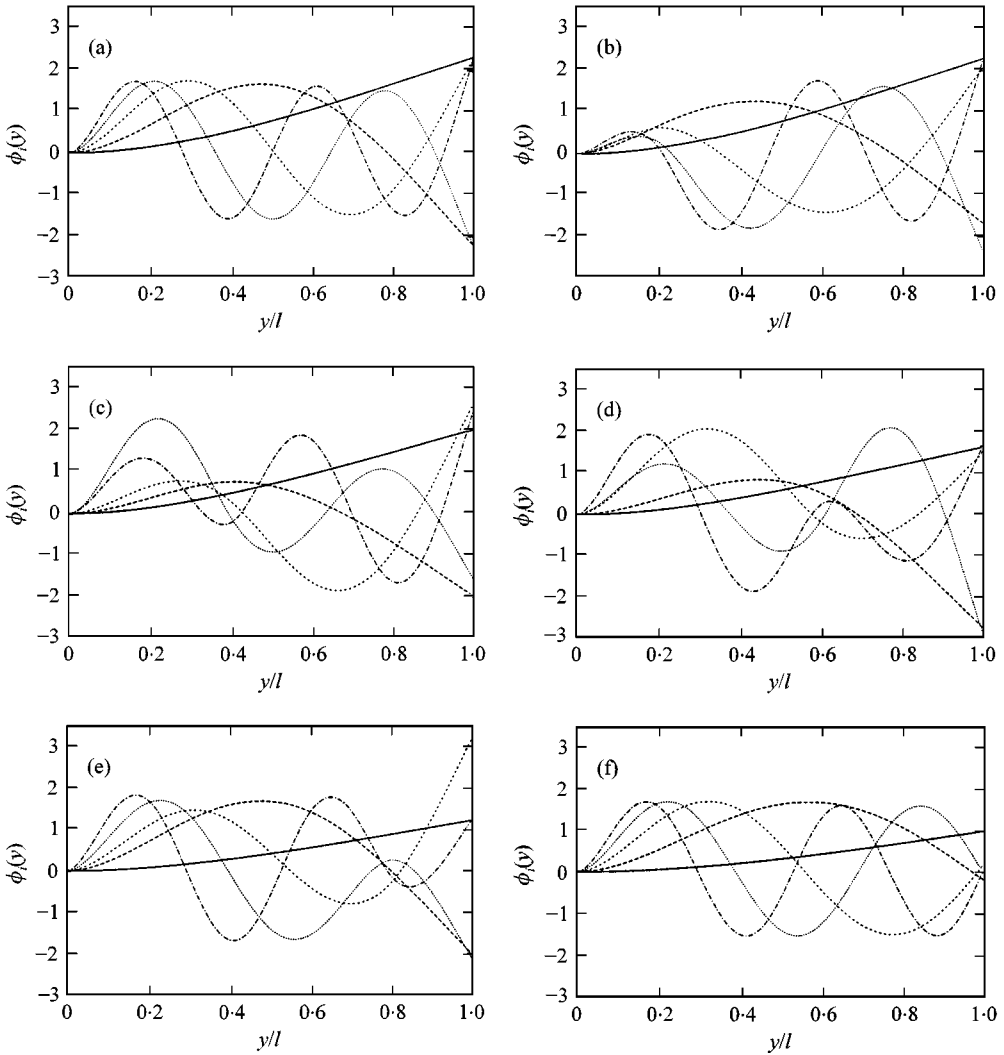
Figure 5. Five normalized mode shapes corresponding to the first five roots of the frequency equation (31) with respect to the change of the position of the concentrated mass at $M = 10$kg, $m = 1$kg, $m_b = 0.788$kg, and $l = 1$m: (a) $h = 0$m, (b) $h = 0.2$m, (c) $h = 0.4$m, (d) $h = 0.6$m, (e) $h = 0.8$m, (f) $h = 1$m. ——, $\phi_1(y)$; −− $\phi_2(y)$; − − −, $\phi_3(y)$; ·····, $\phi_4(y)$; − · − ·, $\phi_5(y)$.

TABLE 2

System parameters

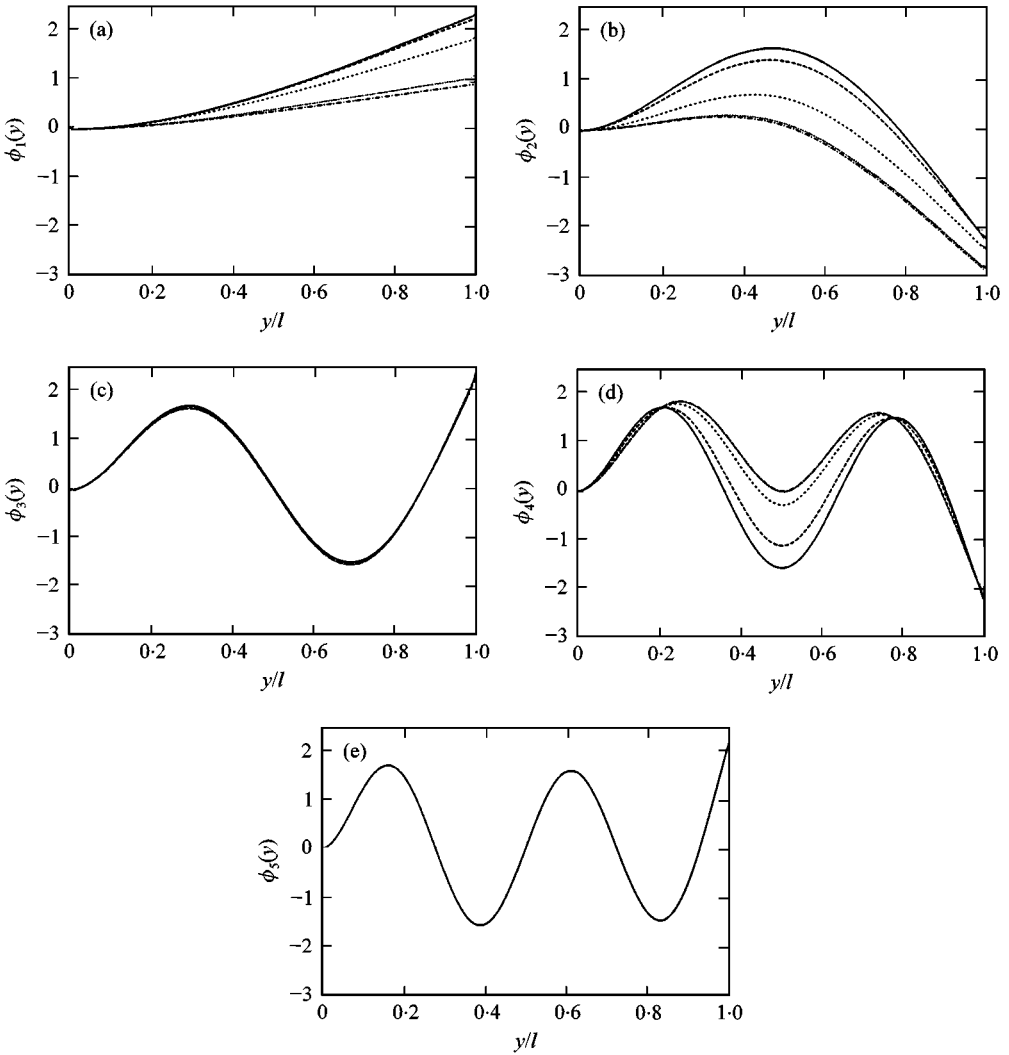| Parameters	Value
Mass of cart, M	10·0 kg
Length of elastic beam, l	1·0 m
Mass per unit length of elastic beam, ρ_0	0·788 kg/m
Young's modulus of elastic beam, E	2.07×10^{11} N/m^2
Area moment of inertia of elastic beam, I	5.208×10^{-11} m^4

Figure 6. Five normalized mode shapes corresponding to the first five roots of the frequency equation (31) with respect to the change of the concentrated mass at $M = 10$kg, $m_b = 0.788$kg, $l = 1$m and $h = 0.5$m: (a) the first modes, (b) the second modes, (c) the third modes, (d) the fourth modes, (e) the fifth modes. ——, $m = 0$kg; – – $m = 0.1$kg; - - -, $m = 1$kg; ·····, $m = 10$kg; – · – ·, $m = 20$kg.

roots of the frequency equation (31) with respect to the changes in concentrated mass when the mass is attached at $h/l = 0.5$. The concentrated mass, m, was changed from 0 to 20 kg, and the system parameters listed in Table 2 were used in the calculation. As shown in Figure 6, mode shapes are changed considerably as the concentrated mass varies. However, the third and the fifth mode shapes are changed little because the nodal points of the third and the fifth modes near $h/l = 0.5$ are 0.51 and 0.5 respectively.

3.4. A SPECIAL CASE

All the equations developed in the previous three subsections work well even in extreme cases where the lumped mass is concentrated at the tip, $h = l$, or bottom, $h = 0$, of the beam. When $m = 0$, however, $A(y)$ in equation (21) and C in equation (26) vanish, and thus D in the equation becomes 1. The condition

$$D - 1 = 0 \qquad (35)$$

gives the fourth frequency equation in Table 1, but it also makes it impossible to compute equations (29) and (34). This problem can be avoided by the following two methods. The first one is letting the mass of the cart be $M - m$ and putting the position of the concentrated mass, m, at the bottom, $h = 0$, of the beam. This method gives the same results as with the fourth system in Figure 1. The other method is letting $m = \varepsilon$ where ε is a positive infinitesimal value and putting the mass at any value in $0 \leqslant h \leqslant l$.

Table 3 shows the first five k_i and β_i by the above two methods respectively. As shown in Table 3, the difference between the two methods is negligible.

3.5. BEAM DEFLECTIONS

Substituting equations (14) and (32) into equation (12) and multiplying both sides of the resulting equation by $\phi_j(y)$ and integrating over the problem domain, one obtains

$$\sum_{i=1}^{\infty} [\ddot{q}_i(t) + \omega_i^2 q_i(t)] \int_0^l \rho(y)\psi_i(y)\phi_j(y)\,\mathrm{d}y = -\ddot{\alpha}(t) \int_0^l \rho(y)\phi_j(y)\,\mathrm{d}y. \qquad (36)$$

Since equation (10) can be rewritten as

$$\beta_j = -\frac{1}{M_t} \int_0^l \rho(y)\phi_j(y)\,\mathrm{d}y, \qquad (37)$$

TABLE 3

Comparison of the first five k_i and β_i for (a) $M = 9$ kg, $m = 1$ kg *and* $h/l = 0$ *with* (b) $M = 10$ kg, $m = 0.00001$ kg *and* $h/l = 1$

i	(a)		(b)	
	k_i	β_i	k_i	β_i
1	1·896696	− 0·066232	1·896672	− 0·066232
2	4·711149	− 0·037850	4·711089	− 0·037850
3	7·864662	− 0·022430	7·864562	− 0·022430
4	11·002652	− 0·016095	11·002513	− 0·016095
5	14·142709	− 0·012542	14·142530	− 0·012543

substitution of equations (9) and (37) into equation (36), for $i = j$, leads to

$$\ddot{q}_i(t) + \omega_i^2 q_i(t) = f(t)\beta_i, \tag{38}$$

for $i = 1, 2, \ldots, \infty$. Then, $q_i(t)$ is obtained by integrating equation (38) for given ω_i and applied force, $f(t)$.

For given $\psi_i(y)$, β_i and $q_i(t)$, the beam deflection is given as

$$w(y, t) = \sum_{i=1}^{\infty} \phi_i(y)q_i(t) = \sum_{i=1}^{\infty} [\psi_i(y) - \beta_i]q_i(t), \tag{39}$$

and accordingly, the position of the cart is given as

$$x(t) = \alpha(t) + \sum_{i=1}^{\infty} \beta_i q_i(t). \tag{40}$$

For simulation purpose, we need assumed-mode solutions as shown in the next subsection.

3.6. ASSUMED–MODE METHOD

Assumed-mode solutions for a finite number of eigenvalues are obtained from previous development by considering the first n terms of equations (39) and (40). The deflection of the elastic beam and the displacement of the cart are expressed, respectively, in terms of n mode shapes using the obtained $\psi_i(y)$, β_i and $q_i(t)$ as follows:

$$w(y, t) = \sum_{i=1}^{n} [\psi_i(y) - \beta_i] q_i(t) \tag{41}$$

and

$$x(t) = \alpha(t) + \sum_{i=1}^{n} \beta_i q_i(t). \tag{42}$$

Now, the inhomogeneous equations (1)–(3) can be transformed into a set of $n + 1$ second-order ordinary differential equations of the form

$$\begin{pmatrix} M_t & 0 \\ 0 & I \end{pmatrix} \begin{pmatrix} \ddot{\alpha} \\ \ddot{q}_i \end{pmatrix} + \begin{pmatrix} 0 & 0 \\ 0 & K \end{pmatrix} \begin{pmatrix} \alpha \\ q_i \end{pmatrix} = \begin{pmatrix} 1 \\ \beta_i \end{pmatrix} f(t), \tag{43}$$

for $i = 1, \ldots, n$, where $K = \text{diag}\{\omega_i^2\}$ is an $n \times n$ *stiffness matrix*. This equation is solved by the fourth order Runge–Kutta method for arbitrarily given forcing function $f(t)$.

4. NUMERICAL SIMULATIONS

   Numerical simulations were carried out to examine the open-loop responses of the system to an arbitrarily designed forcing function. The parameters listed in Table 2 are used in the simulations.

   Figure 7 shows the global position of cart, $x(t)$, the global tip position of the beam, $x_T(t)$, the global position of the concentrated mass, $x_h(t)$, the local deflection where the concentrated mass is attached, $w_h(t)$, and the local deflection at the tip of the beam, $w_T(t)$, respectively, where $x_T(t) = x(t) + w_T(t)$, $x_h(t) = x(t) + w_h(t)$, $w_h(t) = w(h\,t)$, and $w_T(t) = w(l, t)$, when the concentrated mass is 1 kg, the mode

Figure 7. The open-loop responses to an arbitrarily designed forcing function when $m = 1kg$: (a) $h/l = 0$, (b) $h/l = 0.2$, (c) $h/l = 0.4$, (d) $h/l = 0.6$, (e) $h/l = 0.8$, (f) $h/l = 1$. —, $x(t)$; $--$, $x_T(t)$; $---$, $x_h(t)$; $\cdots$, $w_h(t)$; $-\cdot-\cdot$, $w_T(t)$.
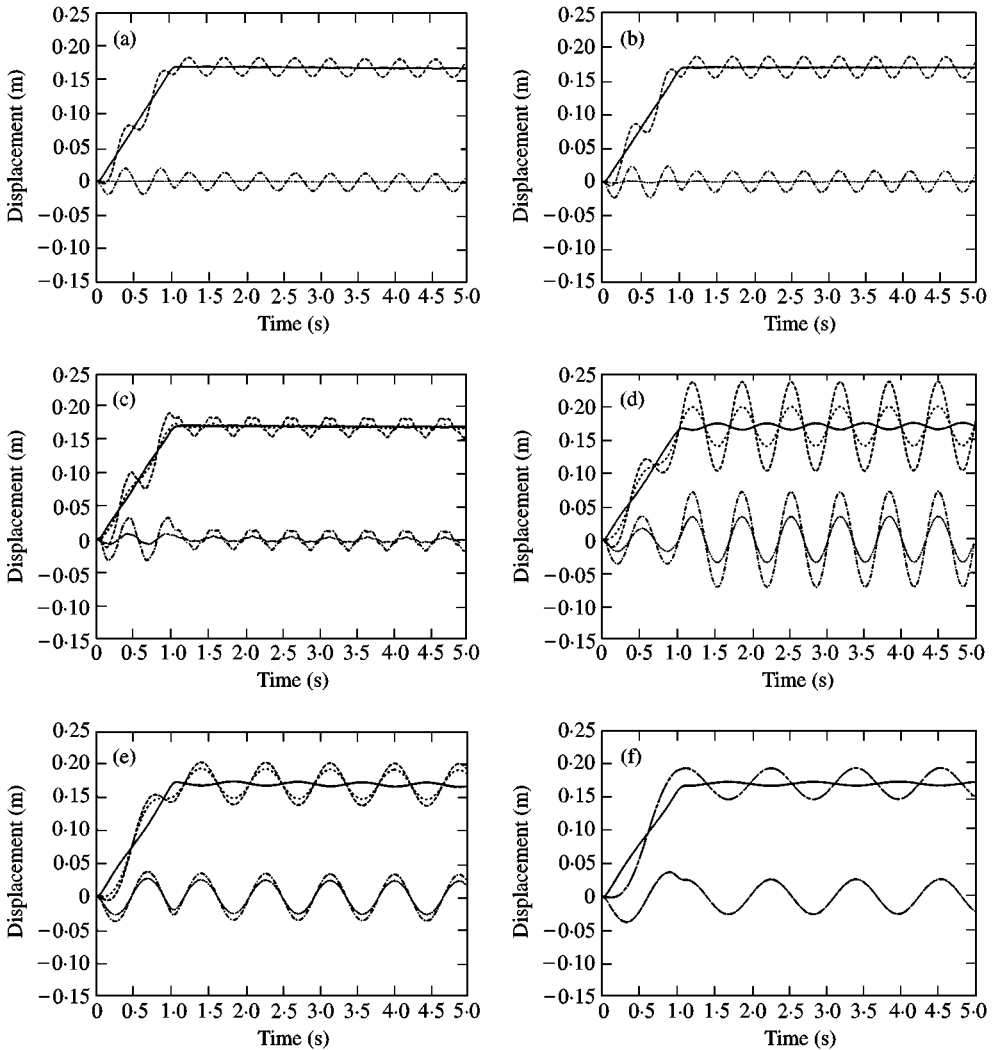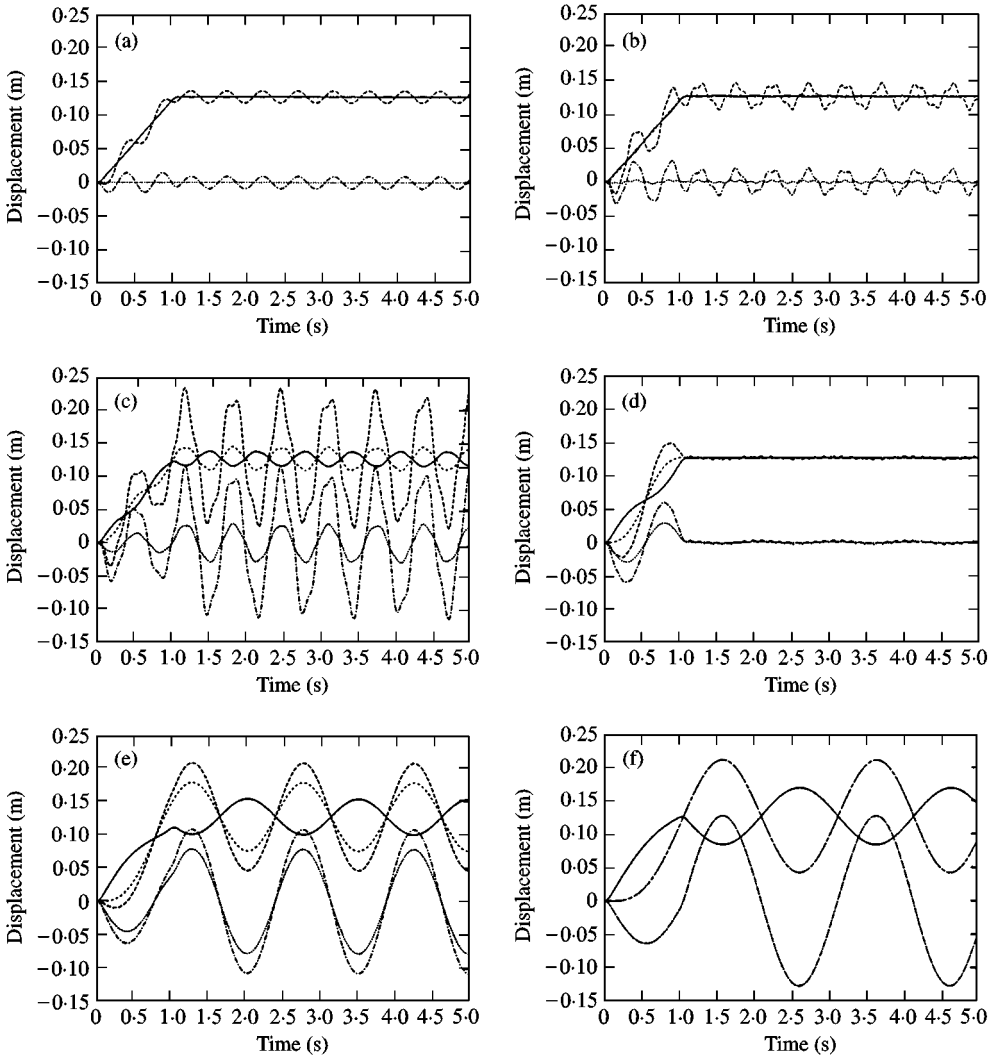
Figure 8. The open-loop responses to an arbitrarily designed forcing function when $m = 5kg$: (a) $h/l = 0$, (b) $h/l = 0.2$, (c) $h/l = 0.4$, (d) $h/l = 0.6$, (e) $h/l = 0.8$, (f) $h/l = 1$. —, $x(t)$; – –, $x_T(t)$; - - -, $x_h(t)$; ·····, $w_h(t)$; – · – ·, $w_T(t)$.

number n is 3, and the following forcing function is applied:

$$f(t) = \begin{cases} 20\,\text{N} & \text{when } 0 < t \leqslant 0\cdot1, \\ -20\,\text{N} & \text{when } 1\cdot0 < t \leqslant 1\cdot1, \\ 0\,\text{N} & \text{otherwise.} \end{cases}$$

Figure 8 shows the results of simulations for the same conditions with the previous simulations except that $m = 5$ kg. In both figures it is natural that $x_h(t)$ coincides with $x(t)$ when $h = 0$ because $w(0, t) = 0$, and that $w_T(t)$ and $x_T(t)$ coincide with $w_h(t)$ and $x_h(t)$ respectively, when $h = l$.

Through these analyses of motion, one can easily notice that not only the position of the lumped mass but also the mass ratios affect the vibrational motion of the beam–mass–cart system. Furthermore, the motion of the concentrated mass and the flexible beam affect that of the cart, and the amplitude of the initial deflection of the beam is proportional to the lumped mass and to the position of the mass, h, as shown in Figures 7 and 8. It is noteworthy that the deflection $w_h = 0$ regardless of the magnitude of the concentrated mass when $\eta = 0$, i.e., $h = 0$ as seen in Figures 7(a) and 8(a) although the natural frequencies are a little different from each other.

The vibration generated at the beam by the applied force is amplified or damped out according to the natural frequency and to the instance of time when the external force is applied. For example, when $m = 5$ kg and $h/l = 0 \cdot 4$, the fundamental frequency of the beam–mass–cart system is $1 \cdot 562$ Hz, and thus when time t is around 1 s, the tip of the vibrating beam starts to return to the neutral point from a backwardly deflected position, and at this time the force applied to the opposite direction amplifies the vibrational motion of the beam. On the contrary, when $h/l = 0 \cdot 6$, the fundamental frequency of the system is $0 \cdot 995$ Hz. Thus, when the time t is around 1 s, the tip of the vibrating beam returns to the neutral point from a forwardly deflected position. Therefore, the vibration of the beam is damped out by the force applied to the opposite direction at this time.

The control method utilizing this concept is the *input-preshaping method*. To suppress the residual vibration of the elastic beam, the frequency characteristics of the beam is important for determining the instance of time to apply the external force [37]. Therefore, the results obtained in this study is helpful for the design of the model-based controller to reduce the vibration of the beam–mass–cart system. The method of analysis introduced in this study can also be used as a dynamic simulator for this kind of beam–mass–cart systems.

5. CONCLUSIONS

In this paper, a Bernoulli–Euler beam fixed on a moving cart and carrying a concentrated mass attached at an arbitrary position along the beam was considered and the equations of motion which describe the global motion as well as the vibrations motion derived. A unified frequency equation which can be generally applied to this kind of beam–mass system was also obtained. The validity of the frequency equation was verified with a vast number of comparative studies. Some roots of the frequency equation were found for various conditions of system parameters. It was shown that the eigenfrequencies and the corresponding mode shapes change considerably as the mass ratios and the position of the concentrated mass vary. The exact and assumed-mode solutions were also obtained by unconstrained modal analysis for the beam–mass–cart system. Finally, the open-loop responses, global motions of the beam–mass–cart system as well as the vibrational motions of the beam by an arbitrary forcing function, were obtained by numerical simulations. This analysis of motion based on system dynamics gives useful information for the design of the vibration suppression controller for the system.

ACKNOWLEDGMENT

REFERENCES

1. R. BHAT and H. WAGNER 1976 *Journal of Sound and Vibration* **45**, 304–307. Natural frequencies of a uniform cantilever with a tip mass slender in the axial direction.
2. G. L. ANDERSON 1978 *AIAA Journal* **16**, 281–282. Natural frequencies of a cantilever with an asymmetrically attached tip mass.
3. L. A. PARNELL and M. H. COBBLE 1976 *Journal of Sound and Vibration* **44**, 499–511. Lateral displacement of a vibrating cantilever with a concentrated mass.
4. P. A. A. LAURA, J. L. POMBO and E. A. SUSEMIHL 1974 *Journal of Sound and Vibration* **37**, 161–168. A note on the vibrations of a clamped-free beam with a mass at the free end.
5. M. GÜRGÖZE 1986 *Journal of Sound and Vibration* **105**, 443–449. On the approximate determination of the fundamental frequency of a restrained cantilever beam carrying a tip heavy body.
6. M. GÜRGÖZE 1996 *Journal of Sound and Vibration* **190**, 149–162. On the eigenfrequencies of a cantilever beam with attached tip mass and a spring mass system.
7. Y. CHEN 1963 *Transaction of American Society of Mechanical Engineers Journal of Applied Mechanics* **39**, 310–311. On the vibration of beams or rods carrying a concentrated mass.
8. R. P. GOEL 1973 *Transaction of American Society of Mechanical Engineers Journal of Applied Mechanics* **40**, 821–822. Vibrations of a beam carrying a concentrated mass.
9. R. P. GOEL 1976 *Journal of Sound and Vibration* **47**, 9–14. Free vibrations of a beam–mass system with elastically restrained end.
10. C. L. AMBA-RAO 1966 *The Journal of the Acoustical Society of America* **40**, 367–371. Method of calculation of frequencies of partially fixed beams carrying masses.
11. H. H. PAN 1965 *Transaction of American Society of Mechanical Engineers Journal of Applied Mechanics* **32**, 434–437. Transverse vibration of an Euler beam carrying a system of heavy bodies.
12. M. M. STANIŠIĆ and J. C. HARDIN 1969 *Journal of the Franklin Institute* **287**, 115–123. On the response of beams to an arbitrary number of concentrated moving mass.
13. M. J. MAURIZI and P. M. BELLÉS 1991 *Journal of Sound and Vibration* **150**, 330–334. Natural frequencies of the beam–mass system: comparison of the two fundamental theories of beam vibrations.
14. M. J. MAURIZI and P. M. BELLÉS 1992 *Journal of Sound and Vibration* **154**, 182–186. An additional evaluation of free vibrations of beam–mass systems.
15. K. H. LOW 1998 *Journal of Sound and Vibration* **215**, 381–389. On the eigenfrequencies for mass loaded beams under classical boundary conditions.
16. L. LIBRESCU and S. S. NA 1997 *Journal of Acoustical Society of America* **102**, 3516–3522. Vibration and dynamic response control of cantilevers carrying externally mounted stores.
17. C. W. S. TO 1982 *Journal of Sound and Vibration* **83**, 445–460. Vibration of a cantilever beam with a base excitation and tip mass.
18. S. S. GE, T. H. LEE and G. ZHU 1998 *IEEE/ASME Transactions on Mechatronics* **3**, 138–144. Asymptotically stable end-point regulation of a flexible SCARA/Cartesian robot.
19. S. D. PARK, W. K. CHUNG, Y. YOUM and J.W. LEE 1998 *Proceedings of Korean Automatic Control Conference (KACC), Pusan, Korea*, 367–372. Analysis of the motion of a cart with an inverted flexible beam and a concentrated tip mass.

20. E. Garcia and D. J. Inman 1991 *Journal of Guidance* **14**, 736–742. Modeling of the slewing control of a flexible structure.
21. K. H. Low 1987 *Journal of Robotic Systems* **4**, 435–456. A systematic formulation of dynamic equations for robot manipulators with elastic links.
22. K. H. Low 1997 *Journal of Sound and Vibration* **204**, 823–828. A note on the effect of hub inertia and payload on the vibration of a flexible slewing link.
23. A. Ankarali and H. Diken 1997 *Journal of Sound and Vibration* **204**, 162–170. Vibration control of an elastic manipulator link.
24. E. H. K. Fung and Z. X. Shi 1997 *Journal of Sound and Vibration* **204**, 259–269. Vibration frequencies of a constrained flexible arm carrying an end mass.
25. E. Barbieri and Ü. Özgüner 1988 *Transaction of Dynamic System Measurement and Control* **110**, 416–421. Unconstrained and constrained mode expansion for a flexible slewing link.
26. L. Meirovitch 1980 *Computational Methods in Structural Dynamics*, MD: Sijthoff & Noordhoff.
27. C. C. De Wit, B. Siciliano and G. Bastin 1996 *Theory of Robot Control*, 219–230. Berlin: Springer-Verlag.
28. W. H. Liu and C.-C. Huang 1988 *Journal of Sound and Vibration* **123**, 31–42. Free vibration of a restrained beam carrying concentrated masses.
29. N. G. Stephen 1982 *Journal of Sound and Vibration* **83**, 585–587. Note on the combined use of Dunkerley's and Southwell's method.
30. M. Gürgöze 1984 *Journal of Sound and Vibration* **96**, 461–468. A note on the vibrations of restrained beams and rods with point masses.
31. M. N. Hamdan and N. H. Shabeneh 1997 *Journal of Sound and Vibration* **199**, 711–736. On the large amplitude free vibrations of a restrained uniform beam carrying an intermediate lumped mass.
32. M. N. Hamdan and M. H. F. Dado 1997 *Journal of Sound and Vibration* **206**, 151–168. Large amplitude free vibrations of a uniform cantilever beam carrying an intermediate lumped mass and rotary inertia.
33. R. D. Blevins 1979 *Formulas for Natural Frequency and Mode Shapes*, 108–109. New York: Van Nostrand Reinhold Co.
34. D. A. Grant 1978 *Journal of Sound and Vibration* **57**, 357–365. The effect of rotary inertia and shear deformation on the frequency and normal mode equations of uniform beams carrying a concentrated mass.
35. R. S. Ayre, L. S. Jacobsen and C. S. Hsu 1951 *Proceedings of the first U.S. National Congress of Applied Mechanics*, 81–90. Transverse vibration of one- and of two-span beams under the action of a moving mass load.
36. G. B. Chai and K. H. Low 1993 *Journal of Sound and Vibration* **160**, 161–166. On the natural frequencies of beams carrying a concentrated mass.
37. C. L. Teo, C. J. Ong and M. Xu 1998 *Journal of Sound and Vibration* **211**, 157–177. Pulse input sequence for residual vibration reduction.

APPENDIX A: PROOF OF EQUATION (33)

Using equation (32), equation (14) can be represented as

$$EI\psi_i''''(y) - \omega_i^2 \rho(y)\psi_i(y) = 0. \tag{A.1}$$

By equation (11), equation (A.1) is rewritten as follows:

$$EI\phi_j''''(y) - \omega_j^2 \rho(y)\phi_j(y) - \omega_j^2 \rho(y)\beta_j = 0. \tag{A.2}$$

The eigenfunction $\psi_i(y)$ is not *self-adjoint* by inhomogeneous boundary conditions in equation (15). However, the eigenfunctions $\phi(y)$ and $\psi(y)$ satisfy

$$\int_0^l \psi_i''''(y)\phi_j(y)\,\mathrm{d}y = \int_0^l \psi_i(y)\phi_j''''(y)\,\mathrm{d}y - \psi_i(y)\phi_j'''(y)\Big|_0^l$$

$$= \int_0^l \psi_i(y)\phi_j''''(y)\,\mathrm{d}y + \frac{M\omega_j^2}{EI}\beta_i\beta_j. \tag{A.3}$$

The boundary conditions in equations (15) and (25) were used in equation (A.3).

Multiplying both sides of equation (A.1) by $\phi_j(y)$, integrating over the problem domain and applying equation (A.3) to the resulting equation, one obtains

$$\int_0^l \left[EI\psi_i''''(y) - \omega_i^2\rho(y)\psi_i(y)\right]\phi_j(y)\,\mathrm{d}y$$

$$= EI\int_0^l \psi_i(y)\phi_j''''(y)\,\mathrm{d}y - \omega_i^2\int_0^l \rho(y)\psi_i(y)\phi_j(y)\,\mathrm{d}y + M\omega_j^2\beta_i\beta_j. \tag{A.4}$$

Multiplying equation (A.2) by $\psi_i(y)$ and integrating the resulting equation from 0 to l yields

$$\int_0^l \left[EI\phi_j''''(y) - \omega_j^2\rho(y)\phi_j(y) - \omega_j^2\rho(y)\beta_j\right]\psi_i(y)\,\mathrm{d}y$$

$$= EI\int_0^l \psi_i(y)\phi_j''''(y)\,\mathrm{d}y - \omega_i^2\int_0^l \rho(y)\psi_i(y)\phi_j(y)\,\mathrm{d}y + M\omega_j^2\beta_i\beta_j. \tag{A.5}$$

because

$$\beta_i = -\frac{1}{M}\int_0^l \rho(y)\psi_i(y)\,\mathrm{d}y \tag{A.6}$$

from equations (10) and (32).

Subtracting equation (A.5) from equation (A.4) becomes 0 as follows because equations (A.1) and (A.2) are the same.

$$(\omega_i^2 - \omega_j^2)\int_0^l \rho(y)\psi_i(y)\phi_j(y)\,\mathrm{d}y = 0. \tag{A.7}$$

Therefore, for $i \neq j$, one can have

$$\int_0^l \rho(y)\psi_i(y)\phi_j(y)\,\mathrm{d}y = 0. \tag{A.8}$$

APPENDIX B. PROOF OF EQUATION (34)

From equations (26) and (29), the following equation is obtained:

$$\phi(y) = \psi(y) - \beta = \psi(h)\left[F(y) - \frac{C}{1-D}\right].\tag{B.1}$$

Utilizing equations (29), (32) and (B.1), the following equation is obtained:

$$\int_0^l \rho(y)\psi_i(y)\phi_j(y)\,dy = m\psi_i(h)\phi_j(h) + \rho_0\int_0^l \psi_i(y)\phi_j(y)\,dy$$

$$= m\psi_i(h)\left[\psi_j(h) - \frac{C_j}{1-D_j}\psi_j(h)\right] + \rho_0\int_0^l \psi_i(h)F_i(y)\psi_j(h)\left[F_j(y) - \frac{C_j}{1-D_j}\right]dy.\tag{B.2}$$

For $i = j$, the left-hand side of equation (B.2) becomes 1 by equation (33). This gives

$$1 = \psi_i^2(h)\left\{\left[m\left(1 - \frac{C_i}{1-D_i}\right)\right] + \rho_0\int_0^l F_i(y)\left[F_i(y) - \frac{C_i}{1-D_i}\right]dy\right\}.\tag{B.3}$$

Thus, equation (34) follows from equation (B.3).